

# Finite element procedure to simulate sandwich structure with an auxetic core under impact loading using ABAQUS/Explicit

Valdo Pratama<sup>1</sup>, Annisa Jusuf<sup>2</sup>, Arief Yudhanto<sup>3,4</sup>, Bambang Kismono Hadi<sup>2</sup>

<sup>1</sup>Aerospace Engineering Study Program, Faculty of Mechanical and Aerospace Engineering, Institut Teknologi Bandung, Bandung, Indonesia

<sup>2</sup>Lightweight Structures Research Group, Faculty of Mechanical and Aerospace Engineering, Institut Teknologi Bandung, Bandung, Indonesia

<sup>3</sup>Mechanical Engineering Program, Physical Sciences, and Engineering Division, King Abdullah University of Science and Technology, Thuwal, Saudi Arabia

<sup>4</sup>Mechanics of Composites for Energy and Mobility Laboratory, King Abdullah University of Science and Technology, Thuwal, Saudi Arabia

## Article Info

### Article history:

Received Sep 19, 2022

Revised Oct 14, 2022

Accepted Dec 7, 2022

### Keywords:

Auxetic

Finite element procedure

Sandwich structure

## ABSTRACT

A sandwich structure with an auxetic core is promising in improving the performance of a sandwich structure by implying an auxetic core as its core to combine the advantages of the two structures, e.g., sandwich structure's superior ability in flexural and shear resistance, auxetic structure in localizing damage, and densification phenomena. This paper discusses a finite element modeling procedure to simulate a sandwich structure with a heterogeneous re-entrant auxetic core. The material of the face is a unidirectional carbon fiber reinforced polymer (UD CFRP) and the core is polylactic acid (PLA). The model is subjected to a low-velocity impact loading and is run through the ABAQUS/Explicit software. We found that the model we developed here could simulate up to the elastic region and identify which element had failed. However, it could not fully resemble and represent the model from reference, where fracture or damage does not occur. This model can be further improved in its material modeling strategy, especially in the fracture modeling of the composite face with compatible material properties in all required sectors, especially damaged sections, which are strictly necessary.

This is an open access article under the [CC BY-SA](https://creativecommons.org/licenses/by-sa/4.0/) license.



## Corresponding Author:

Annisa Jusuf

Lightweight Structures Research Group, Faculty of Mechanical and Aerospace Engineering

Institut Teknologi Bandung

Ganesa Street No. 10, Bandung 40132, Indonesia

Email: annisa.jusuf@itb.ac.id

## 1. INTRODUCTION

The sandwich structure is constructed from a thick core material bonded to the skin materials on its upper and lower sides. The skin material usually has a high stiffness characteristic; this may be obtained by using fiber-laminate composites or high-modulus metals. The core structure can accommodate high compressive and shear strengths. Combining the skin and core will create a sandwich structure with the ability of high flexural modulus due to its high moment of inertia (insertion of material in the structure).

Sandwich structures are commonly used in aeronautics, especially in aircraft (Boeing 787 uses composite sandwich panels as part of the wing skin structure [1]). During the operation, aircraft can fly at both low velocities during landing and approach, and high velocities when taking off and in cruise conditions. With this condition, aircraft are prone to impacting objects during flights, which may cause damage and even

lead to catastrophic events. Added to its disadvantages such as high manufacturing cost and longer manufacture time, we have an incomplete understanding of sandwich structures under impact loading [2].

Core material with a negative poisson ratio (NPR) may contract when it is compressed and expand when it is tensioned [3]. The term “auxetic” was first introduced in 1991 by Kenneth E. Evans [3]. Under low-velocity impact [4]–[11], high-velocity impact [12]–[15], and blast loading [16]–[20], a core with NPR performs better in terms of energy absorption, damage localization, and densification. With such an “auxetic” characteristic, the possibility of increasing the performance of sandwich structures is promising.

Several authors have studied the impact behavior of sandwich structure with an auxetic core. An investigation finds the impact behavior of a composite sandwich structure, where the core is made of aluminum and the plate is made of steel, with auxetic and honeycomb core geometries under blast loading using finite element software (ABAQUS/Explicit). They found that the auxetic core was better at localizing the stress distribution, where the deformation concentrates towards the impacts area, than the honeycomb core due to the auxetic behavior [16].

Others investigated the low-velocity impact behavior of carbon-fiber-reinforced plastic (CFRP) sandwich panels with various geometries of auxetic and non-auxetic cores. They found that the auxetic core increases the impact resistance of sandwich composite due to core densification that reduces the indentation depth. The auxetic core effectively improved impact damage resistance at a higher impact energy level of 76 J, whereas foam core performs better at energy levels lower than 10 J [4].

Studies from researchers worldwide indicate that there is a need and possibilities for better-performing structures for impact mitigations. Research has been done by implementing these auxetic unit cells as their numerical test subjects. The behavior of a 3D re-entrant structure under various crushing velocities. In their study, it is concluded that the auxetic of the structure may have greater energy dissipation when it is given a crushing loading. The energy dissipated increases as the crushing velocity are increased. Densification gives greater strength and higher crushing resistance performance [21].

Others also investigate that auxetic foam as a filler in a square tube under quasi-static compressive loading. These studies compare with conventional positive poisson's ratio (PPR) foam as a filler on the square tube. The result shows that square tubes with auxetic foam filler have higher energy absorption capability and specific energy absorption (SEA) than conventional PPR foam-filled square tubes. These studies found that auxetic structures can mitigate impact loading by densifying their geometry and have better energy absorption abilities through their auxetic characteristics [22].

This paper addresses technical notes on what is important in a finite element procedure to simulate sandwich plates with composite faces and a core with NPR under low-velocity impact. We used ABAQUS/Explicit to develop the models based on [4]. The aim of this work is to develop a model of a sandwich structure with an auxetic core, conduct numerical experiments of sandwich structure with an auxetic core under the low-velocity impact, and compare the result from Usta [4] which uses LS DYNA with this paper's findings. The model is strictly limited to the development of a sandwich model under dynamic (impact) loading using ABAQUS/Explicit software. The materials were CFRP for the faces and polylactic acid (PLA) for the core. We strictly adopted the sandwich dimension from Usta [4].

## 2. RESEARCH METHOD

### 2.1. Finite element method (FEM) modeling strategy

The sandwich structure model was defined according to the geometry and material properties used by Usta *et al.* [4]. The dimension of the face is  $150 \times 100$  mm using a 3D deformable shell with a thickness of 1.05 mm. The heterogeneous core resembles the same dimension in XY-plane and uses a 3D deformable shell with a total core thickness of 24 mm and 0.7 mm thickness for the auxetic cell struts. It is important to note that when creating the heterogeneous auxetic core, when the column height has non-zero decimals, it needs to be made directly as one (1) column and not one (1) unit cell and reproduced in the direction of the row and column. This strategy is to prevent errors when the geometry has meshed. The three-dimensional visualization of the extruded auxetic core is shown in Figure 1.

The material used for the face is UD CFRP consisting of three plies with [0/45/90] orientation and utilizes the composite layup sub-module (see Tables 1 and 2). For the core, PLA polymer is used (see Figure 2 and Table 3). The impactor uses a 3D rigid shell with a hemispherical-end cylinder. The radius dimension of the hemispherical end is 10 mm and 35 mm in the length of the cylinder body. The impactor's mass is 22.5 kg, so the density and mass can adjust with the impactor's geometry as it is a loading media rather than the research interest.

The constraint between the face and core was connected using "Tie Constraint" because we want to model the two components as if they are bonded together. Therefore an adhesive layer is not required to be modeled. However, if the users want to simulate the effect of an adhesive layer, then a different approach can

be made. For the master surface, the surface will be from the face. For the slave surface, the surface will be from the core. The surface of the face in which the constraint is defined is only one connected face-to-face with the heterogeneous auxetic core surfaces. The impactor is constrained as a rigid body with free movements only in Z-axis translation (same direction as the loading direction).

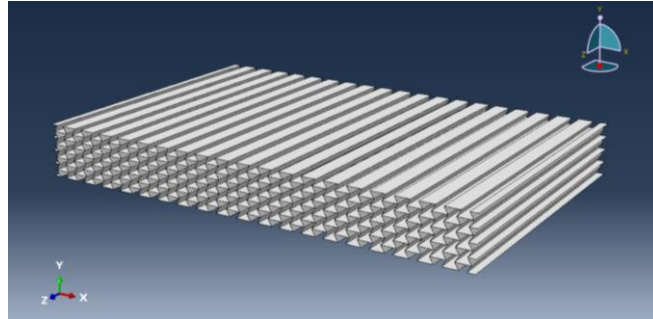


Figure 1. Re-entrant auxetic unit cell whole structure in a three-dimensional (3D) view

Table 1. UD CFRP (elastic and damage properties for lamina [4])

Parameters	Symbols	Value	Units
Elastic Properties (Engineering Constants)			
Density	$\rho$	$1.5 \times 10^{-9}$	tonne/mm <sup>3</sup>
Longitudinal stiffness	$E_{11}$	160 000	MPa
Transversal stiffness	$E_{22}$	6500	MPa
Out-of-plane stiffness	$E_{33}$	6500	MPa
Poisson's ratio	$\nu_{12}$	0.12	-
	$\nu_{13}$	0.12	-
	$\nu_{23}$	0.40	-
Shear modulus	$G_{12}$	5680	MPa
	$G_{13}$	5680	MPa
	$G_{23}$	2840	MPa
Damage Properties			
Longitudinal tensile strength	$X_T$	1020	MPa
Longitudinal compressive strength	$X_C$	650	MPa
Transverse tensile strength	$Y_T$	70	MPa
Transverse compressive strength	$Y_C$	100	MPa
Longitudinal shear strength	$S_L$	80	MPa
Transverse shear strength	$S_T$	80	MPa

Table 2. UD CFRP damage properties (fracture energy) for lamina [23]

Parameters	Symbols	Value	Units
Longitudinal tensile fracture energy	$G_{XT}$	48.4	N/mm
Longitudinal compressive fracture energy	$G_{XC}$	60.3	N/mm
Transverse tensile fracture energy	$G_{YT}$	4.5	N/mm
Transverse compressive fracture energy	$G_{YC}$	8.5	N/mm

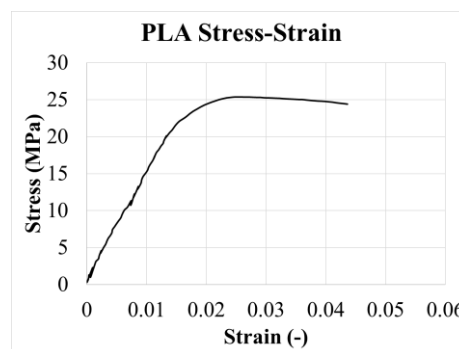


Figure 2. PLA stress-strain curve [4]

Table 3. PLA material properties [4]

Parameters	Symbols	Value	Units
Polylactic Acid Material Properties			
Young's Modulus	E	1900	MPa
Poisson's Ratio	$\nu$	0.36	-
Density	$\rho$	$1.4 \times 10^{-9}$	tonne/mm <sup>3</sup>
Ductile Damage Properties			
Fracture Strain	-	0.02398	-
Stress Triaxiality	-	0.333	-
Strain Rate	$\dot{\epsilon}$	0	s <sup>-1</sup>
Displacement at Failure	-	0.025892	-

The loads are defined by the impactor, a rigid body, and a reference point. The reference point is optional for load definition simplification, where it will couple all the impactor's structure, and the designated velocity will define only the reference point. The simulation is loaded under low-velocity impact with 2.6 m/s or 76 J. The boundary condition on the support implies the ASTM-7136 support configuration with a fixed support type (see Figures 3-5) for the boundary condition configuration). This boundary condition has been proven to avoid a ringing effect on the structure due to overconstrained boundary conditions, where sufficient support is used to hold the structure in place during impact.

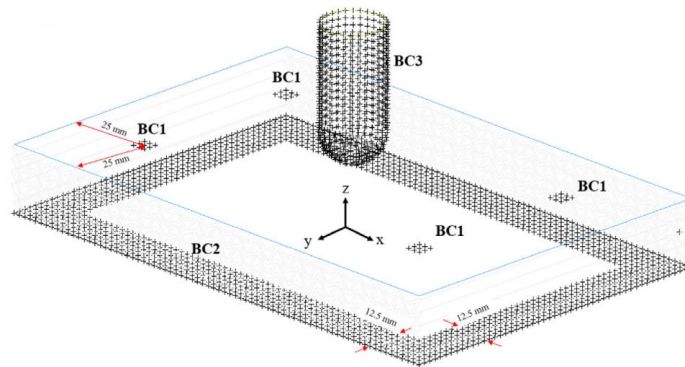


Figure 3. ASTM-7136 boundary condition configuration of simulation [4]

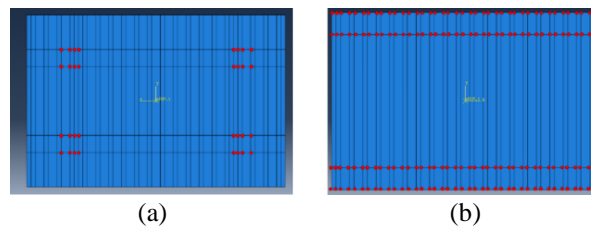


Figure 4. Boundary condition location for (a) the upper face and (b) the lower face, as well as the partition of the part

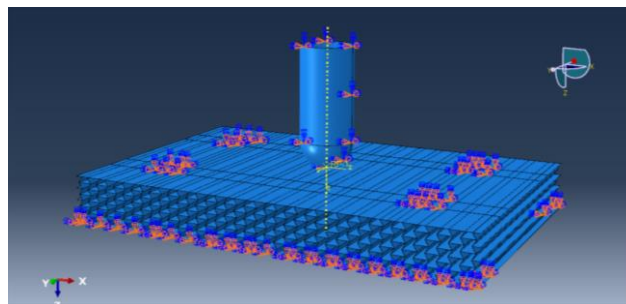


Figure 5. Final visualization of the boundary condition when applied to the model

The meshing uses an S4R element type where the mesh size is 1.25 mm with quad-structured elements. A partition of the face is recommended to connect the mesh between the face and the core. The impactor mesh is coarse as it has already been defined as a rigid body.

The interactions use interaction property where the tangential behavior is defined with "Penalty" in the friction formulation section and a 0.2 friction coefficient. Also, "Hard" contact is chosen in the normal behavior section. The contact type is general contact (explicit) which includes "All" with self" so that when the structure deforms and contacts each other, they will notice neighboring elements and deforms with contact accordingly.

The end time or the simulation is set depending on the units used. In our case, the time is 0.015 seconds (or 15 milliseconds). The step increment can also be selected according to the user's objective. However, in our case, we will not change it and let it be default. The frequency interval of the data saving is also important to record how much data is and at what time the data is stored. The author uses space-time intervals evenly with the interval of 150 to get information for every 0.1 ms. The bigger the interval, the more data is recorded, and the more computer memory is needed.

When using a composite material, to visualize the Hashin damage, damage initiation criteria (DMICRT) will need to be activated for the composite components so that the Hashin damage can be set as an output. The reason is that in ABAQUS/Explicit, the Hashin damage initiation criterion cannot be selected directly in field output. It can only be selected directly in the history output.

## 2.2. Hashin damage initiation criteria

We employed the Hashin damage criterion, a material damage initiation for fiber-reinforced composites. It is based on [8], [9], where the criteria consider four different damage initiation mechanisms, which are fiber tension, fiber compression, matrix tension, and matrix compression. In (1)-(4) show the equation for each damage criterion. Generally, when an initiation criterion has reached a value of 1.0 or higher, the damage initiation has been met, and the damage process will start on the structure.

Fiber tensile

$$\left(\frac{\sigma_{11}}{X^T}\right)^2 + \alpha \left(\frac{\tau_{12}}{S^L}\right)^2 \quad (1)$$

Fiber compression

$$\left(\frac{\sigma_{11}}{X^C}\right)^2 \quad (2)$$

Matrix tensile

$$\left(\frac{\sigma_{22}}{Y^T}\right)^2 + \left(\frac{\tau_{12}}{S^L}\right)^2 \quad (3)$$

Matrix compression

$$\left(\frac{\sigma_{22}}{2S^T}\right)^2 + \left[\left(\frac{Y^C}{2S^T}\right)^2 - 1\right] \left(\frac{\sigma_{22}}{Y^C}\right) + \left(\frac{\tau_{12}}{S^L}\right)^2 \quad (4)$$

Where,  $\sigma_{11}$ ,  $\sigma_{22}$  is the normal stress in direction-1 and -2.  $\tau_{12}$  is the shear stress in plane-1 and direction-2.  $X^T$ ,  $X^C$  is the tensile and compressive strength in the fiber direction.  $Y^T$ ,  $Y^C$  is the tensile and compressive strength in the matrix direction.  $S^L$ ,  $S^T$  is the longitudinal and transversal shear strength.  $\alpha$  is the coefficient for the contribution of shear stress to fiber tensile initiation criteria.

## 2.3. Explicit time integration

The finite element method is used to solve differential equations, especially to find components such as stresses on a structure numerically. In specific, ABAQUS/Explicit uses explicit methods and a central difference method scheme. An explicit method is used as the model is dynamic loading, nonlinearity, and high discontinuity in the solution such as impact or failure simulation, especially in a three-dimensional model. In (5) is the explicit method (6) is the dynamic equilibrium (7) is the central-difference method equation.

$$Y(t + \Delta t) = F(Y(t)) \quad (5)$$

Where,  $Y(t)$  is the current state and  $Y(t + \Delta t)$  is the future or time-step state,  $\Delta t$  is the time-step increment.

$$M\ddot{u} = P - I \quad (6)$$

Where M represents the lumped mass matrix to calculate the accelerations of the nodals, P is the external load, and I is the internal load.

$$\left(\frac{\partial u}{\partial x}\right)_i = \frac{u_{i+1} - u_{i-1}}{2\Delta x} \quad (7)$$

### 3. RESULTS AND DISCUSSION

#### 3.1. Visualization of deformation

The deformation visualization of the sandwich structure for whole and half structures is shown in Figure 6 and Figure 7. The damage progression of the sandwich structure is shown in Figure 8. The maximum deformation is located at the center of the sandwich structure, where the impact occurs. The phenomena of the structure do not visualize the correct behavior where the face made of composite is brittle and should damage upon impact. However, this phenomenon can differ when using different materials, such as metals. The composite material model needs to be re-evaluated.

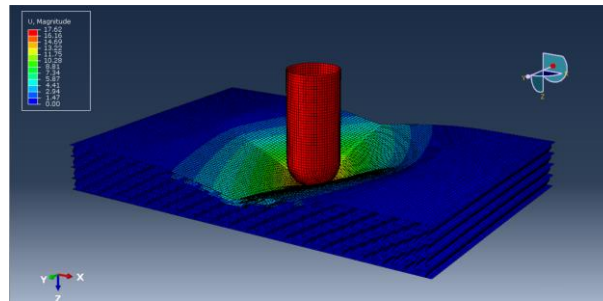


Figure 6. Sandwich structure deformation visualization for the whole structure

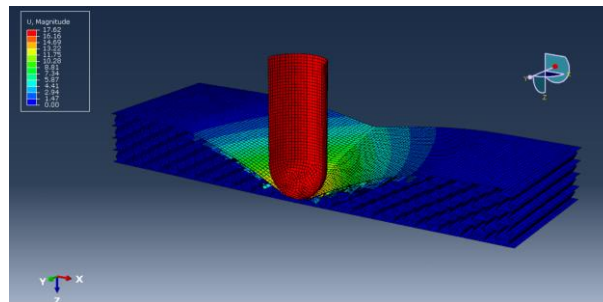


Figure 7. Sandwich structure deformation visualization for half-structure

#### 3.2. Visualization of failure

Hashin damage criteria visualization in fiber-tensile direction is shown in Figure 9. The progression of the damage is shown from 2.0 ms until 11.0 ms range with an increment of 1.0 ms. It can be seen further that some elements have reached the maximum value for the damage criteria (1.0) but have not yet been deleted (in default, damaged elements are deleted). The cause of these findings still needs to be investigated later.

As the simulation time increases, the element also stretches larger than its original size, strengthening the leading hypothesis that there could be a possibility of missing or incorrect damage properties. Thus, the result does not show how composite panels under impact loading should be. In ABAQUS/Explicit, the Hashin damage model requires fracture energy properties which from Usta [4] is not available. Therefore, an effort is made to obtain the fracture energy properties. Some references refer to works by Koloor [23] for fracture energy.

The difference in software usage can be discussed as reference [4] uses LS DYNA as the software to investigate their work. However, in this paper, ABAQUS/Explicit is used as the main software. LS DYNA failure uses such failure criteria. Where a damage initiation point is reached, the element will instantly be deleted. This case is incomplete when conducted in the same manner in ABAQUS/Explicit, where damage evolution comes after the damage initiation part, which hence would not instantly delete the element after a damage initiation point is reached. The difficulty arises because damage evolution requires an important property: the material's fracture energy. Incompatibility of all the material properties leads to incorrect and invalid simulation, thus misleading results in the damaged region. It is known that fracture energy is a material property usually obtained from experimental results. Therefore, an initial experimental test is needed for this material's properties to get a more precise result and data.

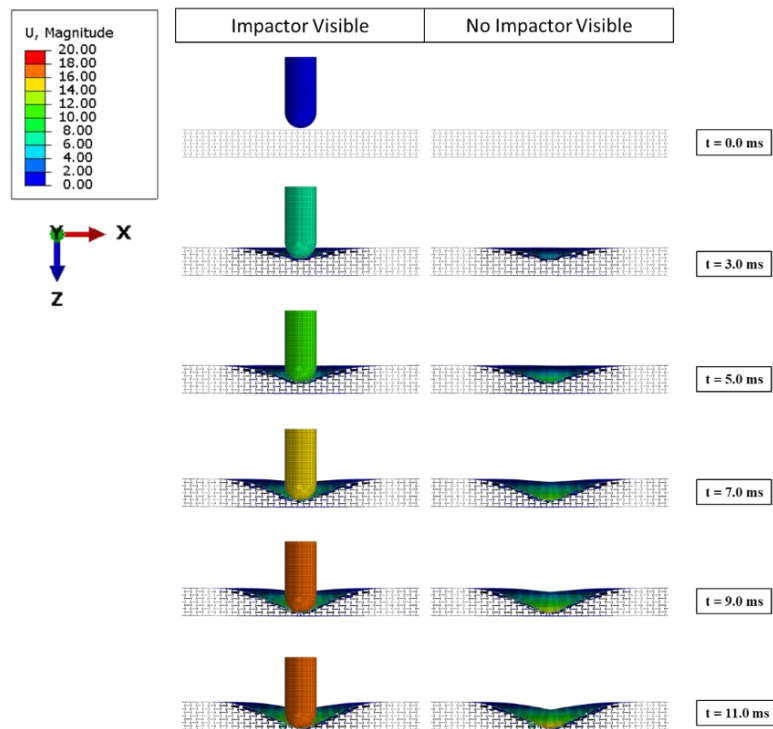


Figure 8. Damage progression of the composite sandwich structure with thermoplastic auxetic core under low-velocity impact loading

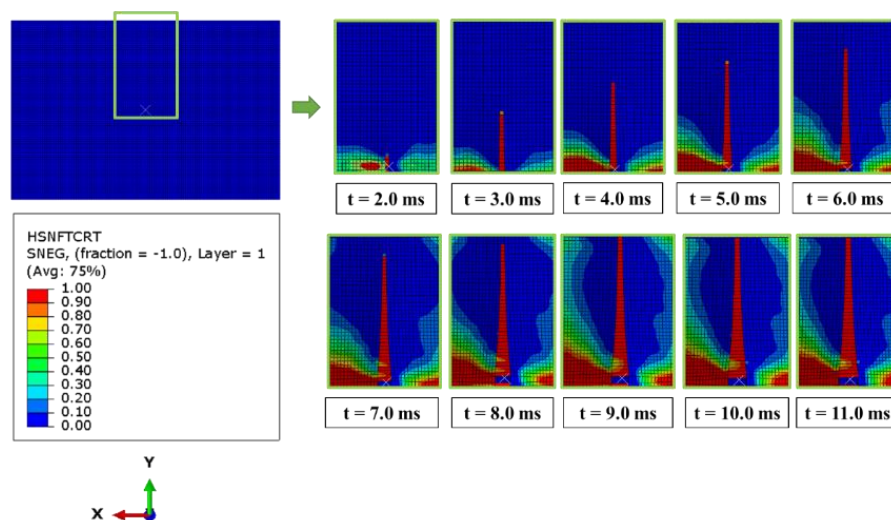


Figure 9. Hashin damage–fiber tensile (DMICRT-HSNFTCRTC) visualization of the composite sandwich panel



### 3.3. Plotting displacement, velocity, and acceleration

The graph showing the displacement, velocity, and acceleration of the impactor is shown in Figures 10-12, respectively. This correlates with the basic principles of impact mechanics. Whereas the displacement increase, the velocity decreases, and the acceleration decreases, hold, and increase to reach zero.

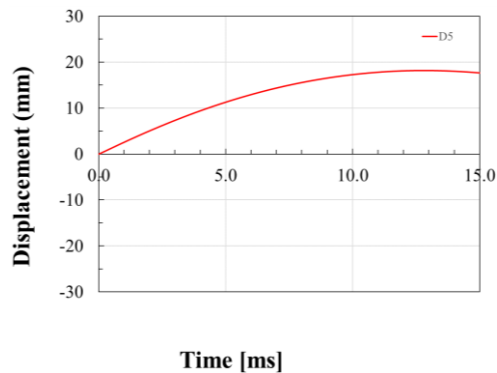


Figure 10. Displacement graph of the impactor

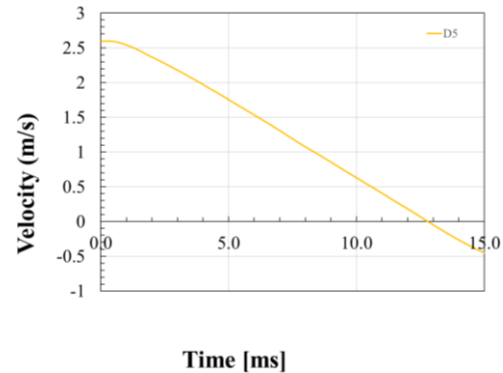


Figure 11. Velocity graph of the impactor

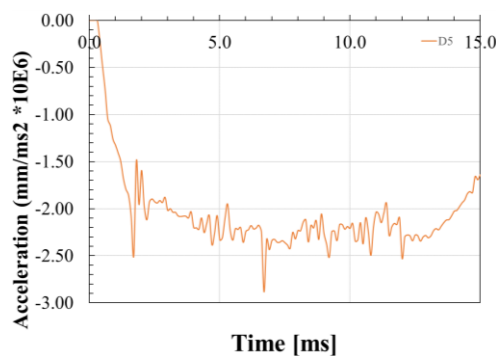


Figure 12. Acceleration graph of the impactor

### 3.4. Plotting force-time and energy diagram

The sandwich structure that the author's model is based on [4]. Therefore, the force-time and force displacement are compared between the author's simulation and the reference data shown in Figure 13 and Figure 14, respectively. However, the energy diagram and the absorbed energy per component are not compared to the reference because the reference does not give information regarding the content. However, the author gives information regarding the total, kinetic, and absorbed energy shown in Figure 15. The absorbed energy per component is also shown in Figure 16.

The result still needs re-evaluation as the behavior does not agree with the real-life behavior. It is discussed in section 3.2 regarding the difference between the simulation of [4] and the findings in this paper. Due to incomplete material property data in all the required sectors, certain obstacles are found, especially in the damaged region. Hence, the difference between this paper's results and reference [4] is acknowledged. Therefore, the objective of this visualization is to give a brief overview that the visualization can be obtained, despite the validity of the numerical value.



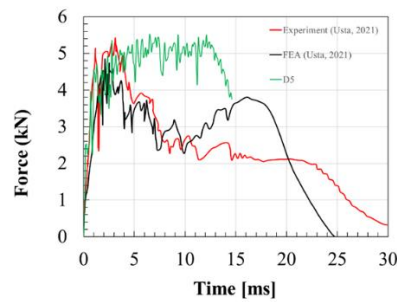


Figure 13. Force-time graph of the sandwich structure

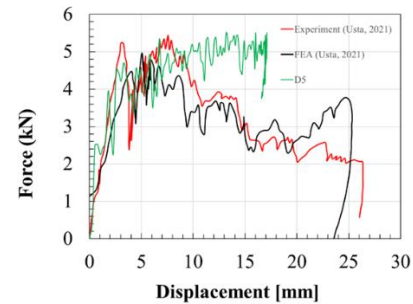


Figure 14. Force-displacement graph of the sandwich structure

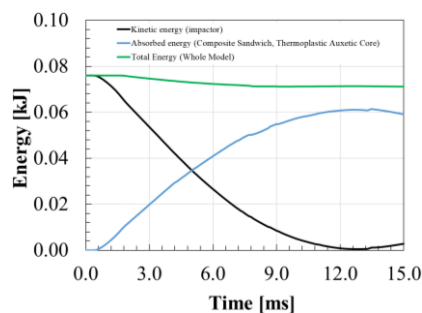


Figure 15. Energy diagram of the sandwich structure

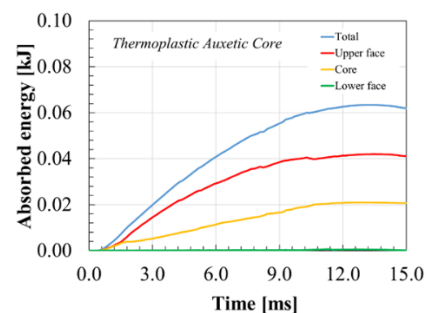


Figure 16. Energy absorbed per component of the sandwich structure

#### 4. CONCLUSION

We provide a finite element procedure to simulate sandwich plates with composite faces and a core with an NPR under low-velocity impact. The model developed here could develop the simulation up to the elastic region. However, it could not fully resemble and represent the model from reference. Further improvements in the material modeling strategy, especially in the fracture modeling of the composite face with compatible material properties in all required sectors, especially damaged sections, are strictly necessary.




#### REFERENCES

- [1] V. Giurgiutiu, "Chapter 1. Introduction," *Structural Health Monitoring of Aerospace Composites*, pp. 1–23, 2016.
- [2] C. Yu, M. Ortiz, and A. J. Rosakis, "3D Modelling of Impact Failure in Sandwich Structures," 2003, pp. 527–537.
- [3] T.-C. Lim, *Auxetic Materials and Structures*. Singapore: Springer Singapore, 2015.
- [4] F. Usta, H. S. Türkmen, and F. Scarpa, "Low-velocity impact resistance of composite sandwich panels with various types of auxetic and non-auxetic core structures," *Thin-Walled Structures*, vol. 163, p. 107738, Jun. 2021, doi: 10.1016/j.tws.2021.107738.
- [5] N. Novak, M. Vesenjak, S. Tanaka, K. Hokamoto, and Z. Ren, "Compressive behaviour of chiral auxetic cellular structures at different strain rates," *International Journal of Impact Engineering*, vol. 141, p. 103566, Jul. 2020, doi: 10.1016/j.ijimpeng.2020.103566.
- [6] G. Imbalzano, P. Tran, T. D. Ngo, and P. V. Lee, "Three-dimensional modelling of auxetic sandwich panels for localised impact resistance," *Journal of Sandwich Structures & Materials*, vol. 19, no. 3, pp. 291–316, May 2017, doi: 10.1177/1099636215618539.
- [7] Y. Shao *et al.*, "Insight into the negative Poisson's ratio effect of the gradient auxetic reentrant honeycombs," *Composite Structures*, vol. 274, p. 114366, Oct. 2021, doi: 10.1016/j.compstruct.2021.114366.
- [8] X. Zhang, H. Ding, L. An, and X. Wang, "Numerical Investigation on Dynamic Crushing Behavior of Auxetic Honeycombs with Various Cell-Wall Angles," *Advances in Mechanical Engineering*, vol. 7, no. 2, p. 679678, Jan. 2015, doi: 10.1155/2014/679678.
- [9] J. Wang, A. M. Waas, and H. Wang, "Experimental and numerical study on the low-velocity impact behavior of foam-core sandwich panels," *Composite Structures*, vol. 96, pp. 298–311, Feb. 2013, doi: 10.1016/j.compstruct.2012.09.002.
- [10] A. Rajaneesh, I. Sridhar, and S. Rajendran, "Impact modeling of foam cored sandwich plates with ductile or brittle faceplates," *Composite Structures*, vol. 94, no. 5, pp. 1745–1754, Apr. 2012, doi: 10.1016/j.compstruct.2011.12.021.
- [11] S. Zhu and G. B. Chai, "Damage and failure mode maps of composite sandwich panel subjected to quasi-static indentation and low velocity impact," *Composite Structures*, vol. 101, pp. 204–214, Jul. 2013, doi: 10.1016/j.compstruct.2013.02.010.
- [12] G. Sun, D. Chen, H. Wang, P. J. Hazell, and Q. Li, "High-velocity impact behaviour of aluminium honeycomb sandwich panels with different structural configurations," *International Journal of Impact Engineering*, vol. 122, pp. 119–136, Dec. 2018, doi: 10.1016/j.ijimpeng.2018.08.007.
- [13] F. Usta, H. S. Türkmen, and F. Scarpa, "High-velocity impact resistance of doubly curved sandwich panels with re-entrant




- honeycomb and foam core,” *International Journal of Impact Engineering*, vol. 165, p. 104230, Jul. 2022, doi: 10.1016/j.ijimpeng.2022.104230.
- [14] D. Xiao, X. Chen, Y. Li, W. Wu, and D. Fang, “The structure response of sandwich beams with metallic auxetic honeycomb cores under localized impulsive loading-experiments and finite element analysis,” *Materials & Design*, vol. 176, p. 107840, Aug. 2019, doi: 10.1016/j.matdes.2019.107840.
- [15] Y. Li, Z. Chen, D. Xiao, W. Wu, and D. Fang, “The Dynamic response of shallow sandwich arch with auxetic metallic honeycomb core under localized impulsive loading,” *International Journal of Impact Engineering*, vol. 137, p. 103442, Mar. 2020, doi: 10.1016/j.ijimpeng.2019.103442.
- [16] G. Imbalzano, S. Linforth, T. D. Ngo, P. V. S. Lee, and P. Tran, “Blast resistance of auxetic and honeycomb sandwich panels: Comparisons and parametric designs,” *Composite Structures*, vol. 183, pp. 242–261, Jan. 2018, doi: 10.1016/j.compstruct.2017.03.018.
- [17] N. Novak, M. Vesenjak, and Z. Ren, “Crush behaviour of auxetic cellular structures,” *Science and Technology of Materials*, vol. 30, no. 1, pp. 4–7, Jan. 2018, doi: 10.1016/j.stmat.2017.12.003.
- [18] F. Arifurrahman, R. Critchley, and I. Horsfall, “Experimental and numerical study of auxetic sandwich panels on 160 grams of PE4 blast loading,” *Journal of Sandwich Structures & Materials*, vol. 23, no. 8, pp. 3902–3931, Nov. 2021, doi: 10.1177/1099636220961756.
- [19] N. Novak, L. Starčević, M. Vesenjak, and Z. Ren, “Blast response study of the sandwich composite panels with 3D chiral auxetic core,” *Composite Structures*, vol. 210, pp. 167–178, Feb. 2019, doi: 10.1016/j.compstruct.2018.11.050.
- [20] C. Qi, A. Remennikov, L.-Z. Pei, S. Yang, Z.-H. Yu, and T. D. Ngo, “Impact and close-in blast response of auxetic honeycomb-cored sandwich panels: Experimental tests and numerical simulations,” *Composite Structures*, vol. 180, pp. 161–178, Nov. 2017, doi: 10.1016/j.compstruct.2017.08.020.
- [21] T. Wang, Z. Li, L. Wang, Z. Ma, and G. Hulbert, “Dynamic Crushing Analysis of a Three-Dimensional Re-Entrant Auxetic Cellular Structure,” *Materials*, vol. 12, no. 3, p. 460, Feb. 2019, doi: 10.3390/ma12030460.
- [22] S. Mohsenizadeh, R. Alipour, A. F. Nejad, M. S. Rad, and Z. Ahmad, “Experimental Investigation on Energy Absorption of Auxetic Foam-filled Thin-walled Square Tubes under Quasi-static Loading,” *Procedia Manufacturing*, vol. 2, pp. 331–336, 2015, doi: 10.1016/j.promfg.2015.07.058.
- [23] S. Rahimian Koor, A. Karimzadeh, N. Yidris, M. Petrú, M. Ayatollahi, and M. Tamin, “An Energy-Based Concept for Yielding of Multidirectional FRP Composite Structures Using a Mesoscale Lamina Damage Model,” *Polymers*, vol. 12, no. 1, p. 157, Jan. 2020, doi: 10.3390/polym12010157.

## BIOGRAPHIES OF AUTHORS






**Valdo Pratama**    is a master's student in Aerospace Engineering at Institut Teknologi Bandung, Indonesia. He received his bachelor's degree in aerospace engineering from Institut Teknologi Bandung in 2021. His research interest includes lightweight structures, composite materials, and impact mechanics. He can be contacted at email: valdo.pratama@gmail.com.






**Annisa Jusuf**    is an associate professor of Aerospace Engineering at the Faculty of Mechanical and Aerospace Engineering, Institut Teknologi Bandung. She received her PhD in 2013 and master's degrees in aerospace engineering from Institut Teknologi Bandung in 2008. Her research interest are experimental and computational impact mechanics, structural design and optimization, and transportation safety. She can be contacted at email: annisa.jusuf@itb.ac.id.



**Arief Yudhanto**    is a research scientist at the Mechanics of Composites for Energy and Mobility Laboratory, King Abdullah University of Science and Technology. He received his PhD in 2013 in aerospace engineering from Tokyo Metropolitan University and master's degree in mechanical engineering from National University of Singapore in 2006. His research interest are in mechanical properties and damage mechanisms in composites, thermoplastic and thermoset composites, 3D stitched and woven composites, progressive damage modeling and homogenization method for composites, composite-based soft actuators, and adhesively-bonded joint of composites. He can be contacted at email: arief.yudhanto@kaust.edu.sa.



**Bambang Kismono Hadi**    is a professor of Aerospace Engineering at the Faculty of Mechanical and Aerospace Engineering, Institut Teknologi Bandung. He received his PhD in 1995 and master's degree in aeronautics from Imperial College London, United Kingdom. His research interest includes experimental and computational mechanics of composite materials and structures. He can be contacted at email: bkhadi@ae.itb.ac.id.